Supplementary Information

Molecular insights into the sensitivity detection mechanism of fluorescent 2D Zr-BTB for 2,4-dinitrophenol

Deyi Zhan [a, b†], Zhiwu Yu [c†], Abdul Saeed [a, b], Qi Hu [a, b], Nanjing Zhao [d], Weihong Xu [a, b*], Junfeng Wang [c*], Lingtao Kong [a*], and Jinhuai Liu [a, b]

[a] *Key Laboratory of Environmental Optics and Technology, and Institute of Solid State Physics, Hefei Institute of Physical Science, Chinese Academy of Sciences, Hefei, Anhui 230031, P. R. China.*

[b] *University of Science and Technology of China, Hefei, Anhui 230031, P. R. China.*

[c] *High Magnetic Field Laboratory, CAS Key Laboratory of High Magnetic Field and Ion Beam Physical Biology, Hefei Institutes of Physical Science, Chinese Academy of Sciences, Hefei, Anhui, 230031, P. R. China.*

[d] *Anhui Institute of Optics and Fine Mechanics, Chinese Academy of Sciences, Hefei 230031, P. R. China.*

†Deyi Zhan and Zhiwu Yu contributed equally to this paper

**Corresponding authors: Tel: +86 551 65595607; Fax: +86 551 65592420;*

E-mail: whxu@iim.ac.cn (W. H. Xu), junfeng@hmfl.ac.cn (J. F. Wang), ltkong@iim.ac.cn (L. T. Kong)

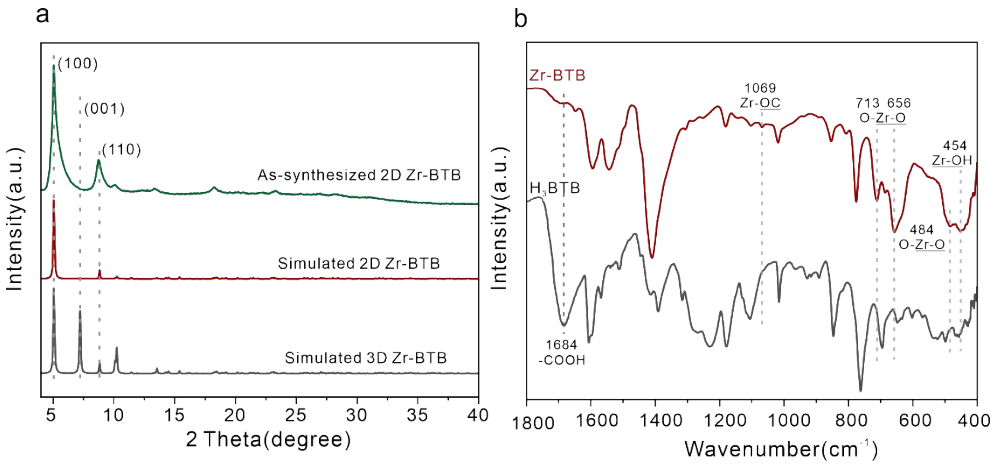

Figure S1. (a) PXRD patterns of as-synthesized product and simulated 2D and 3D Zr-BTB. (b) FTIR spectra of ligand H_3BTB and as-synthesized 2D Zr-BTB nanosheets.

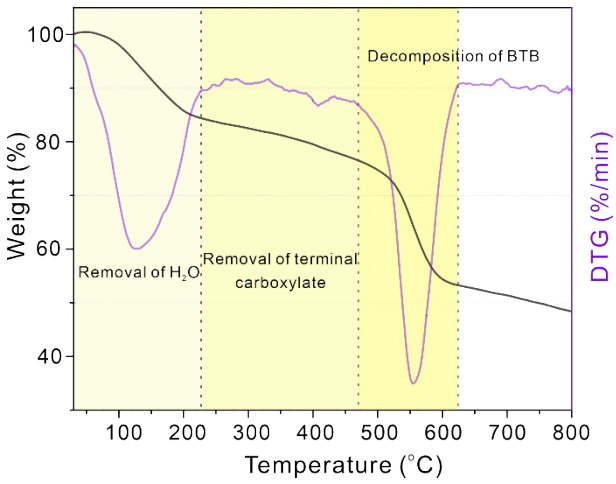

Figure S2. TGA of as-synthesized 2D Zr-BTB nanosheets.

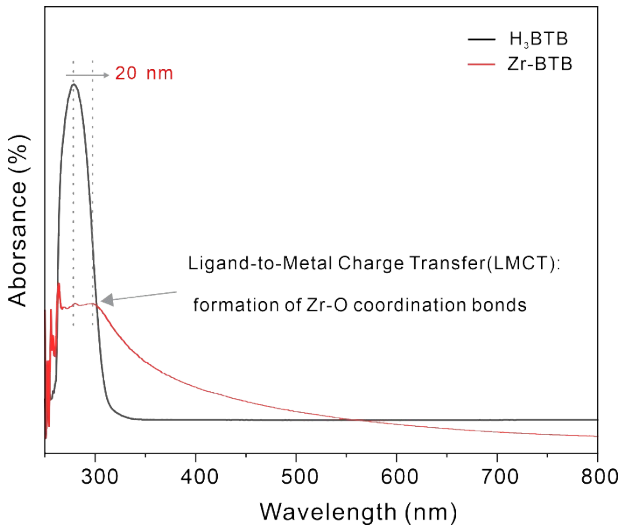

Figure S3. UV-vis absorption spectra of ligand H_3BTB and 2D Zr-BTB nanosheets.

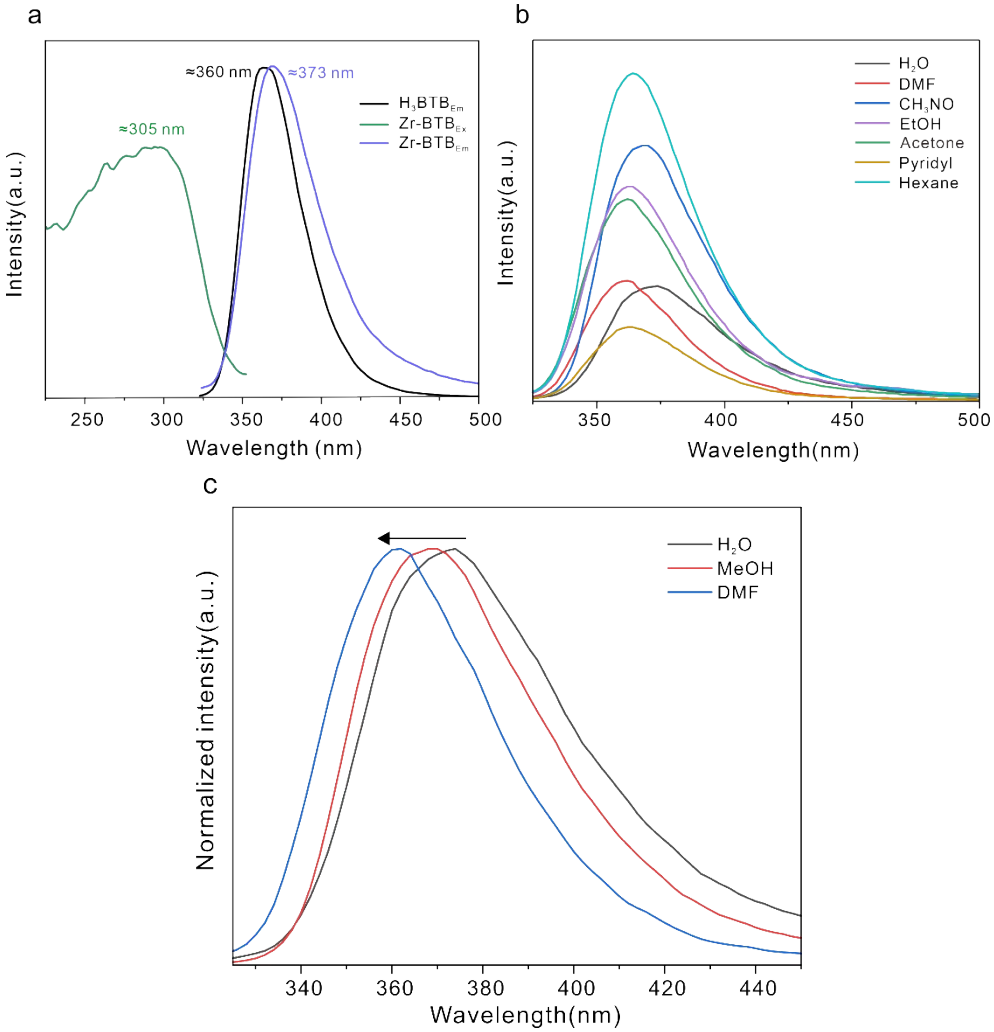

Figure S4. (a) The emission spectrum of H_3BTB, and excitation and emission spectra of 2D Zr-BTB nanosheets. (b) Emission spectra of Zr-BTB dispersed in various solvents. (c) Normalized intensity of Zr-BTB in H_2O, MeOH, and DMF.

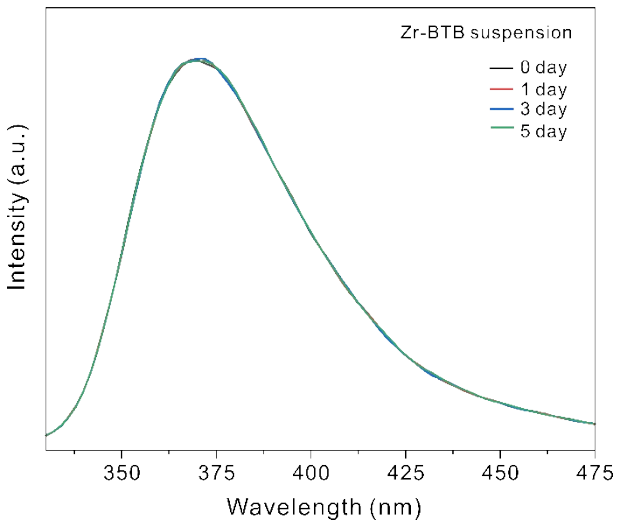

Figure S5. Fluorescence emission spectra of 2D Zr-BTB nanosheets dispersed in water for 0-5 days.

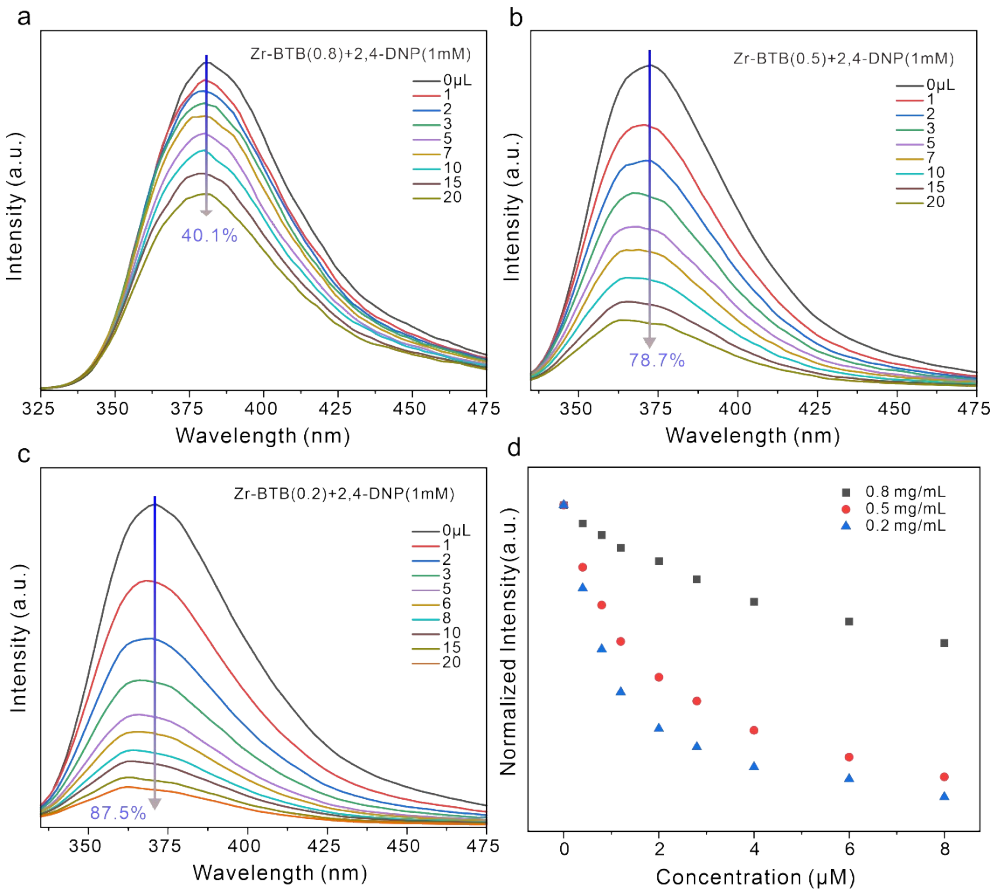

Figure S6. (a-c) Fluorescence emission spectra of 2D Zr-BTB nanosheet suspension with various concentrations (0.8, 0.5, 0.2 mg/mL) by adding different volumes of 1.0 mM of 2,4-DNP. (d) Normalized fluorescence intensity of Zr-BTB suspension in the presence of a different concentration of 2,4-DNP (0-8 μM) at room temperature.

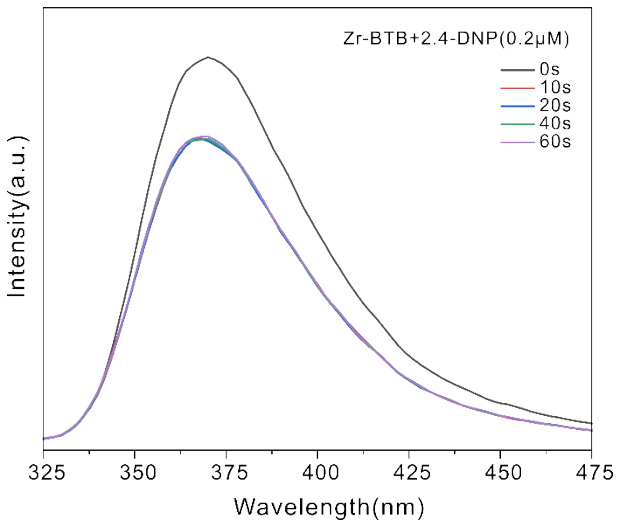

Figure S7. Fluorescence emission of Zr-BTB suspension before and after adding 2,4-DNP of 0.2 μM at 10, 20, 40, and 60 s.

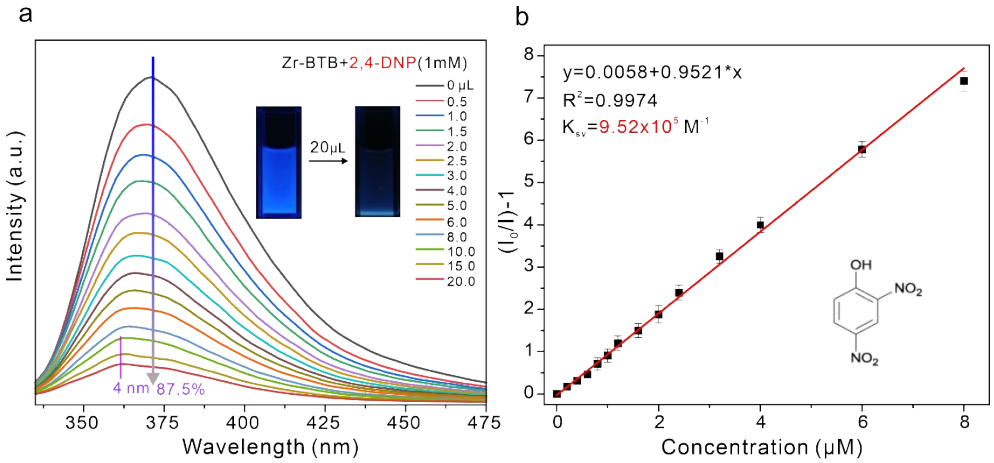

Figure S8. (a) Fluorescence emission spectra of 2D Zr-BTB nanosheets dispersed in water (0.2 mg/mL) upon incremental addition of 2,4-DNP (1mM, 0-20 μL). (b) Corresponding S-V plots of MOF suspension toward 2,4-DNP (0-8 μM).

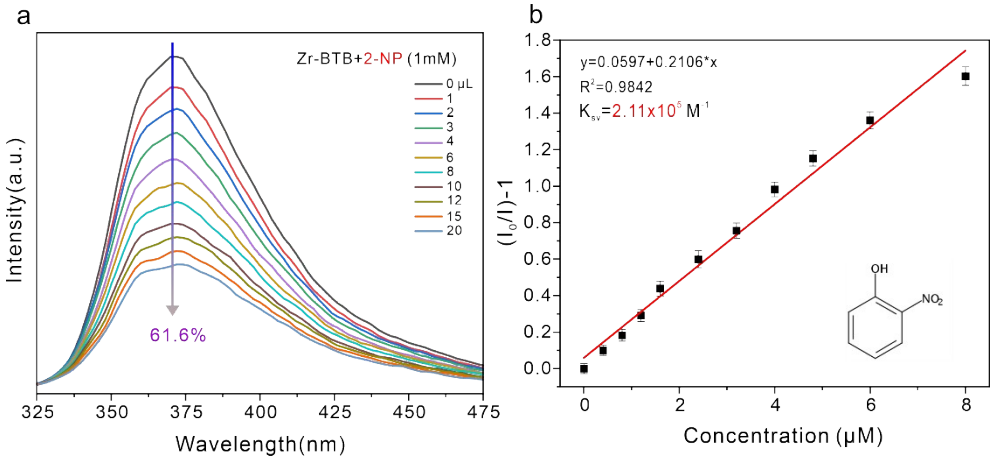

Figure S9. (a) Fluorescence emission spectra of 2D Zr-BTB nanosheets dispersed in water (0.2 mg/mL) upon incremental addition of 2-NP (1mM, 0-20 μL). (b) Corresponding S-V plots of MOF suspension toward 2-NP (0-8 μM).

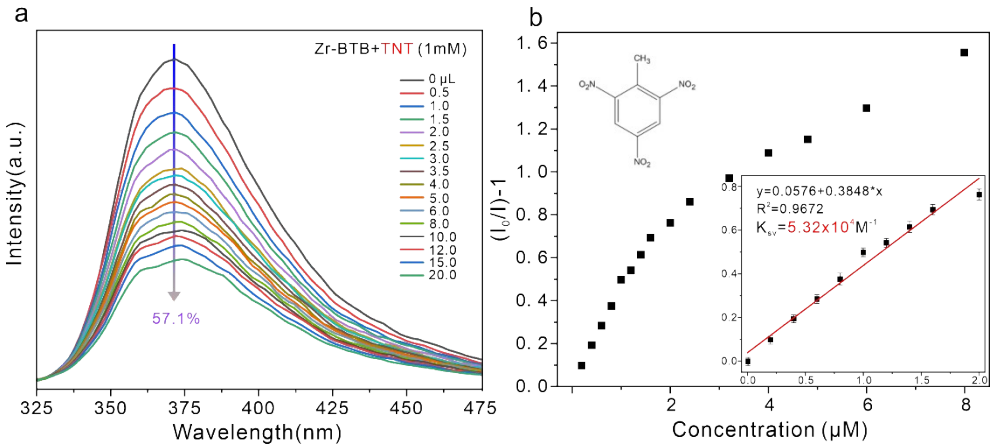

Figure S10. (a) Fluorescence emission spectra of 2D Zr-BTB nanosheets dispersed in water (0.2 mg/mL) upon incremental addition of TNT (1mM, 0-20 μL). (b) Corresponding S-V plots of MOF suspension toward TNT (0-8 μM).

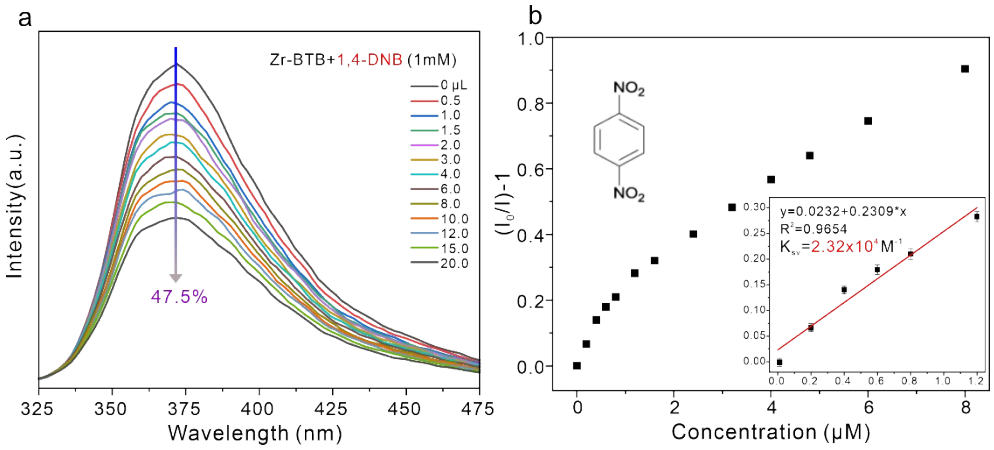

Figure S11. (a) Fluorescence emission spectra of 2D Zr-BTB nanosheets dispersed in water (0.2 mg/mL) upon adding 1,4-DNB (1mM, 0-20 μL). (b) Corresponding S-V plots of MOF suspension toward 1,4-DNB (0-8 μM).

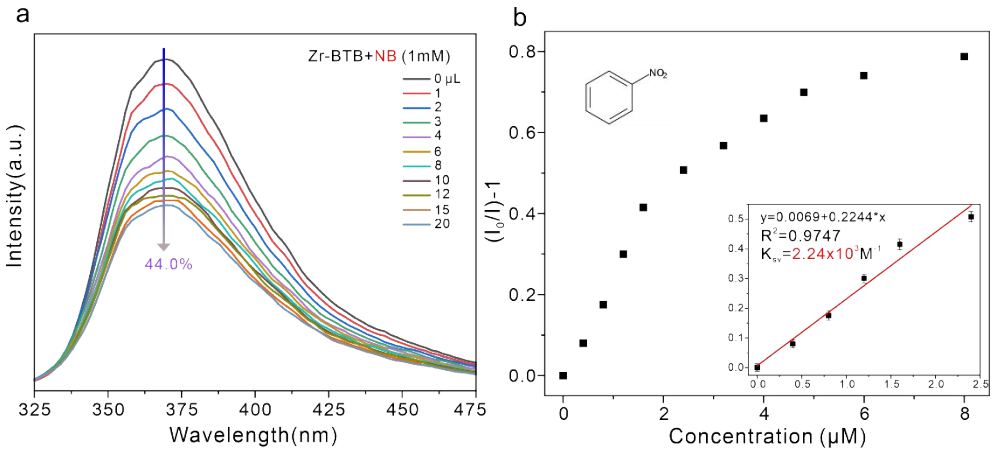

Figure S12. (a) Fluorescence emission spectra of 2D Zr-BTB nanosheets dispersed in water (0.2 mg/mL) upon incremental addition of NB (1mM, 0-20 μL). (b) Corresponding S-V plots of MOF suspension toward NB (0-8 μM).

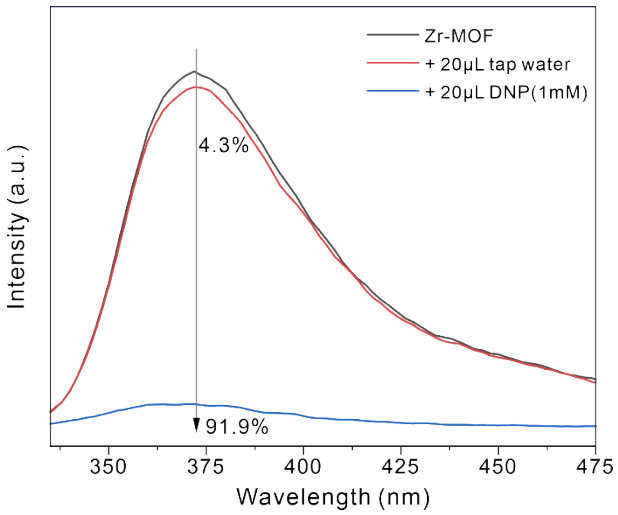

Figure S13. Fluorescence emission spectra of 2D Zr-BTB nanosheets dispersed in water (0.2 mg/mL) upon incremental addition of 20 μL of 2,4-DNP in tap water (1.0 mM).

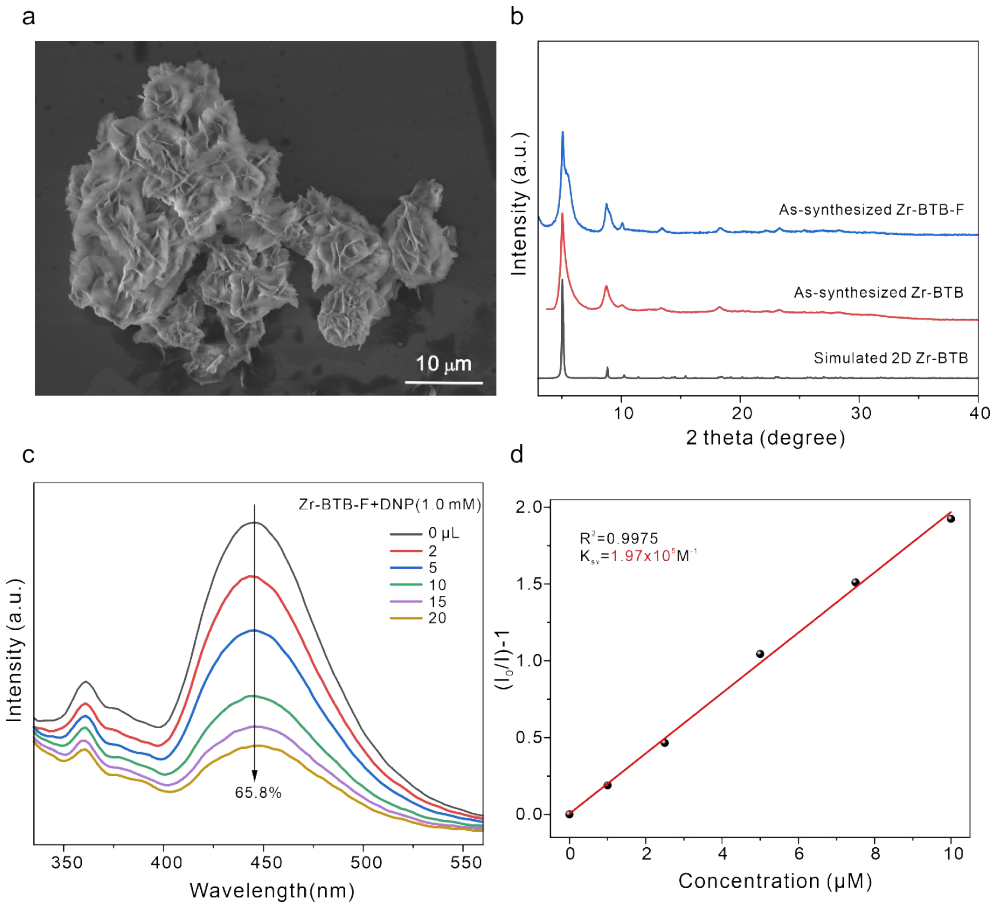

Figure S14. (a) SEM and (b) PXRD of as-synthesized 2D Zr-BTB-F. (c) Fluorescence emission spectra of 2D Zr-BTB-F dispersed in water (0.2 mg/mL) upon incremental addition of 2,4-DNP (1mM, 0-20 μL). (d) Corresponding S-V plots of MOF suspension toward 2,4-DNP (0-8 μM).

The as-synthesized Zr-BTB-F shows an ultrathin morphology with a smooth surface, which is consistent with the morphology of 2D Zr-BTB.[1] The PXRD patterns of both also greatly match well, indicating the same phase. Therefore, Zr-BTB-F is analogous to Zr-BTB. However, the quenching efficiency of Zr-BTB-F towards 2,4-DNP of 8 μM is only 68.5%, significantly lower than that of Zr-BTB (87.5%) under the same conditions. Additionally, the quenching constant K_{sv} for Zr-BTB is 4.8 times higher than that of Zr-BTB-F (K_{sv}=9.52×10^5, 1.97×10^5 M^{-1}, respectively).

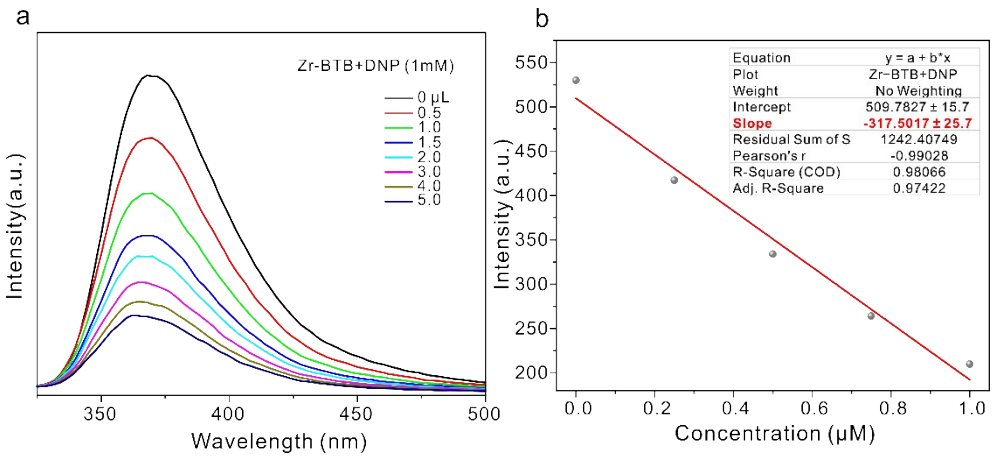

Figure S15. (a) Fluorescence emission spectra, and (b) corresponding fluorescence intensity- analyte concentration (2,4-DNP) plot of MOF suspension (0.2 mg/mL) upon incremental addition of 2,4-DNP (1mM, 0-5 µL).

Limit of Detection (LOD) for 2,4-DNP with 2D Zr-BTB nanosheets in the aqueous phase:

LOD = 3σ/slope [2]

= 3 * 1.38/317.50

= 13.04 nM (2.40 ppb)

Multiple fluorescence spectra (n = 10) were recorded for the blank sample of Zr-BTB suspension. The sample standard deviation σ for the blank probe, without adding 2,4-DNP, was calculated to be 1.38.

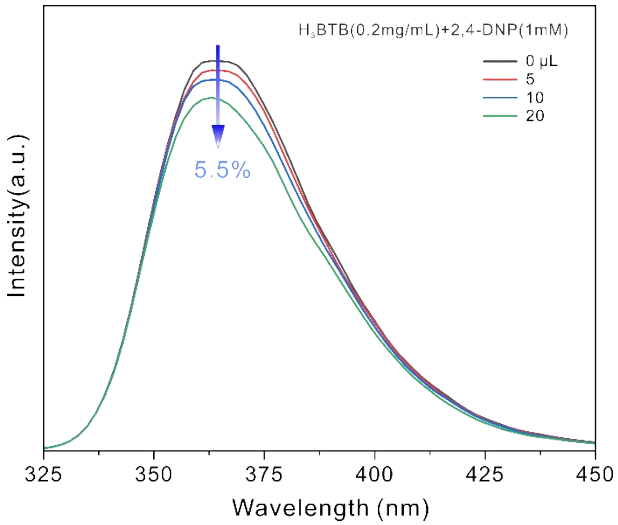

Figure S16. Fluorescence emission spectra of ligand H_3BTB solution (0.2 mg/mL) upon addition of 2,4-DNP (1mM, 0-20 μL).

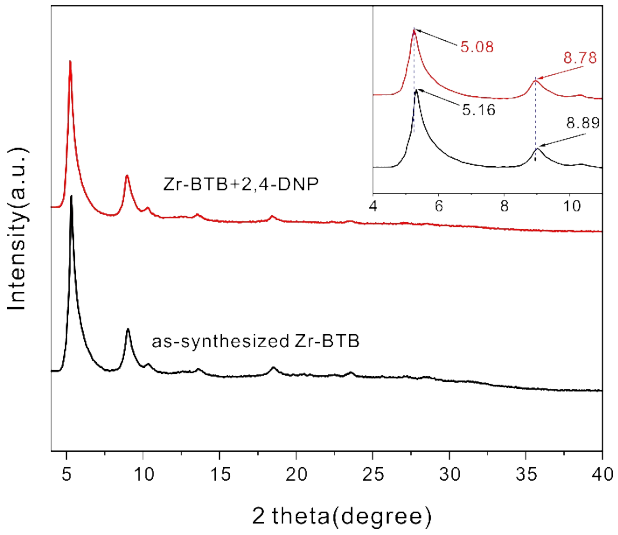

Figure S17. PXRD patterns spectra of Zr-BTB before and after treatment with 8 μM of 2,4-DNP.

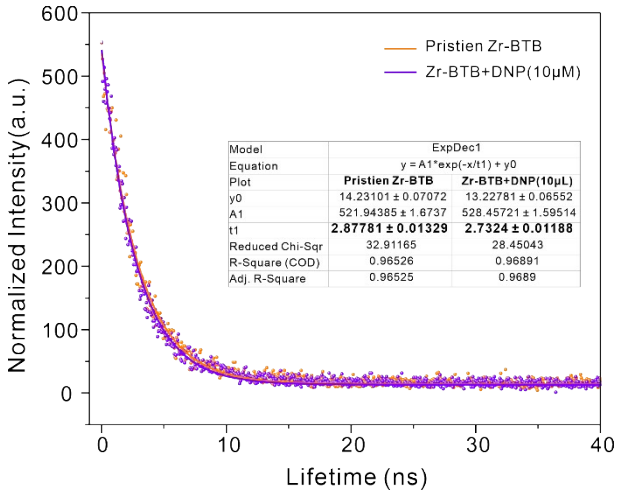

Figure S18. Fluorescence decay curves of Zr-BTB suspension before and after adding 2,4-DNP of 10 μM.

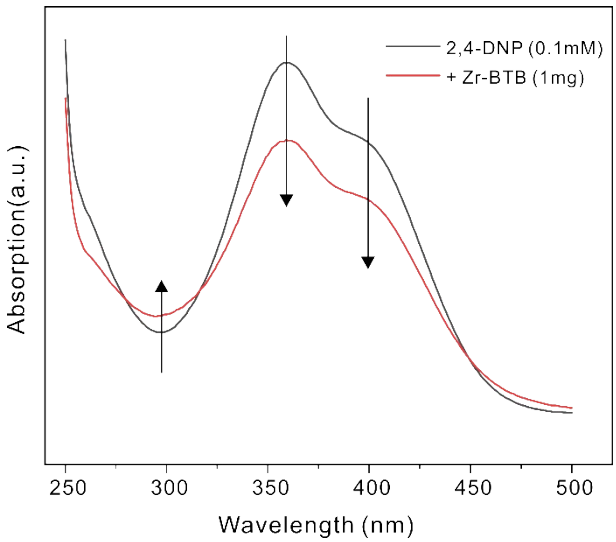

Figure S19. UV-vis absorption spectra of 2,4-DNP (0.1 mM, 2.0 mL) before and after interaction with Zr-BTB (1 mg).

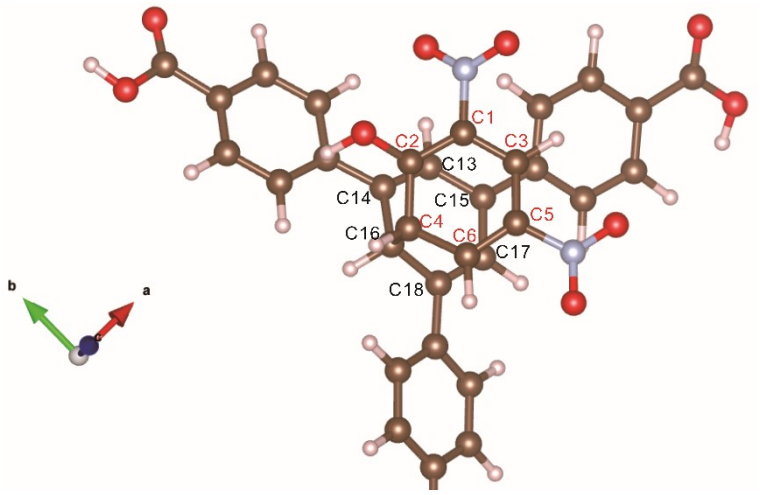

Figure S20. The theoretical modeling of the adsorption I: a π-π stacking interaction of the benzene rings between 2,4-DNP and 2D Zr-BTB.

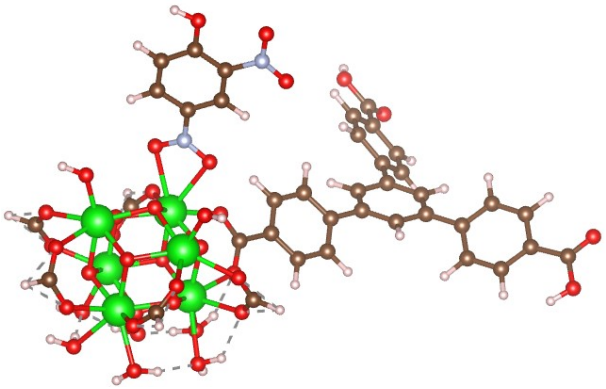

Figure S21. The theoretical modeling of the adsorption II: oxygen atoms from electron-deficient -NO_2 groups coordinated with electron-rich Zr^{4+}.

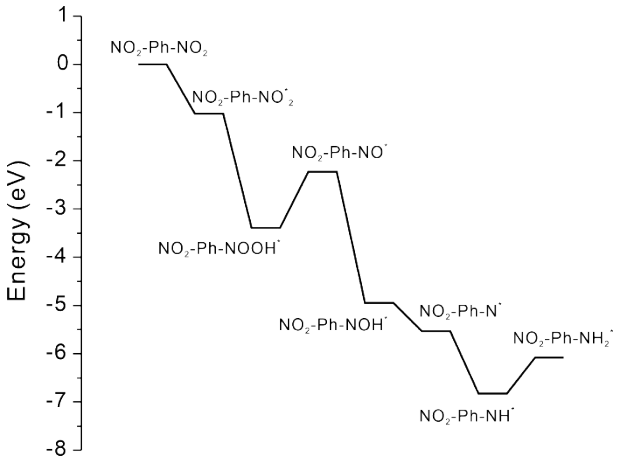

Figure S22. Potential energy surface of NO_2-Ph- NO_2 (2,4-DNP) converted to NH_2-Ph-NO_2.

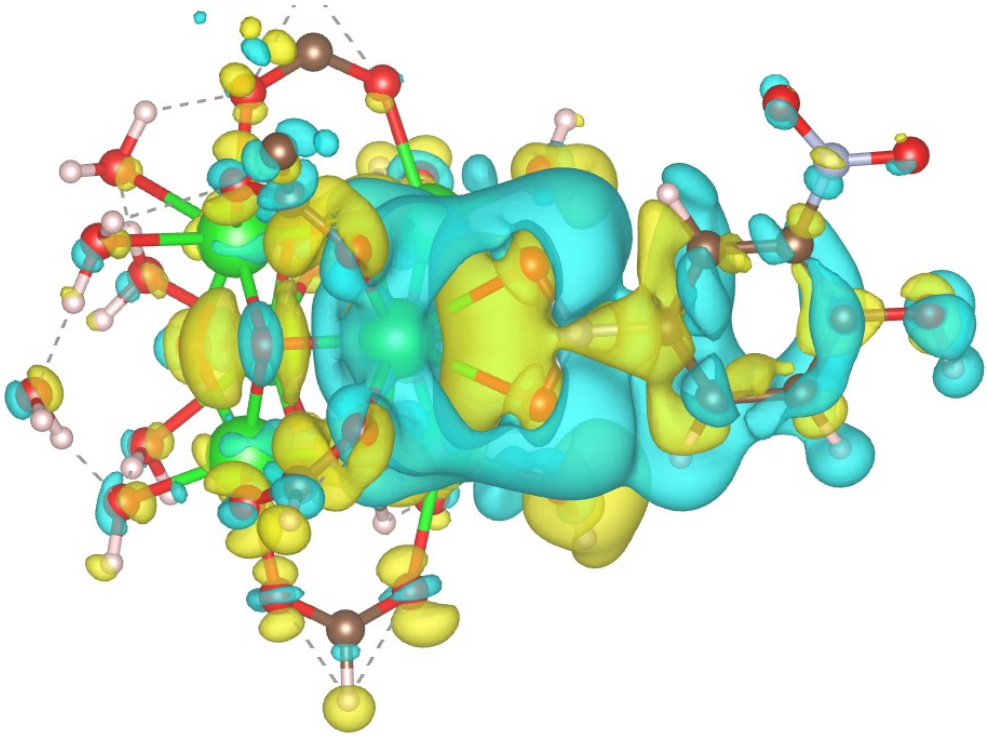

Figure S23. The differential charge density of Zr-BTB after treatment with 2,4-DNP. (Green: Zr; Red: O; Brown: C; Blue: N; White: H. Yellow isosurface: electron accumulation; Cyan isosurface: electron depletion)

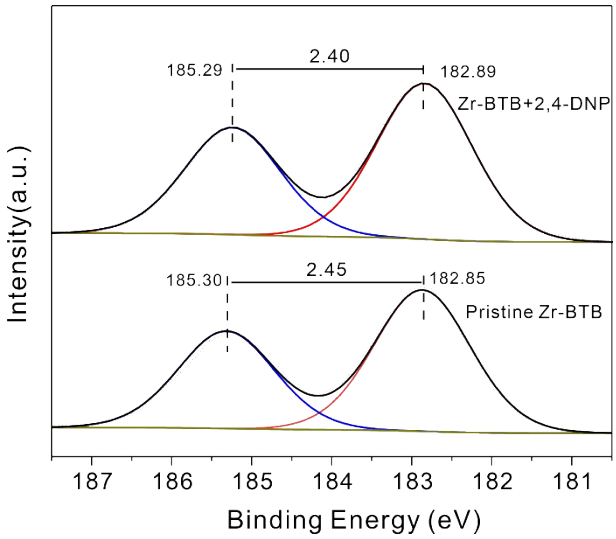

Figure S24. Zr3d of XPS spectrum in pristine Zr-BTB and after treatment with 2,4-DNP of 20 μM.

Table S1. Bader charge of C13-C18 of the benzene ring in Zr-BTB before and after the π-π stacking interaction of MOF with the analyte.

Atomic Number	Pristine Zr-BTB/ Bader Charges	π-π interaction/ Bader Charges
C13	7.234017	4.063068
C14	7.294802	4.047308
C15	7.292674	4.004978
C16	7.295883	3.960551
C17	7.220108	4.080929
C18	4.003895	4.025344

References

1. Y. Wang, L. Feng, J. D. Pang, J. L. Li, N. Huang, G. S. Day, L. Cheng, H. F. Drake, Y. Wang, C. Lollar, J. S. Qin, Z. Y. Gu, T. B. Lu, S. Yuan and H. C. Zhou, *Adv. Sci.*, 2019, **6**, 1802059.
2. J. Yang, Z. Wang, K. L. Hu, Y. S. Li, J. F. Feng, J. L. Shi and J. L. Gu, *ACS Appl. Mater. Interfaces*, 2015, **7**, 11956-11964.